Theses and Dissertations   1. Thesis and Dissertation Collection, all items

1977-06

Analysis of wave/object interaction using distributed source elements of linearly varying strengths.

Williams, Bruce Arnold

Monterey, California. Naval Postgraduate School

http://hdl.handle.net/10945/18019

ANALYSIS OF WAVE/OBJECT INTERACTION
USING DISTRIBUTED SOURCE ELEMENTS OF
LINEARLY VARYING STRENGTHS

Bruce Arnold Williams

NAVAL POSTGRADUATE SCHOOL
Monterey, California

THESIS
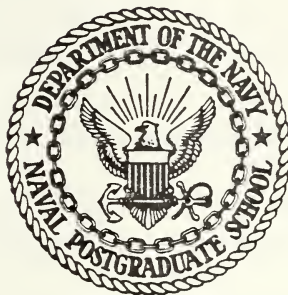
ANALYSIS OF WAVE/OBJECT INTERACTION

USING DISTRIBUTED· SOURCE ELEMENTS OF

LINEARLY VARYING STRENGTHS

by

Bruce Arnold Williams

June 1977

Thesis Advisor: C. J. Garrison

Approved for public release; distribution unlimited.

T180058

REPORT DOCUMENTATION PAGE		READ INSTRUCTIONS BEFORE COMPLETING FORM
1. REPORT NUMBER	2. GOVT ACCESSION NO.	3. RECIPIENT'S CATALOG NUMBER
4. TITLE (and Subtitle) ANALYSIS OF WAVE/OBJECT INTERACTION USING DISTRIBUTED SOURCE ELEMENTS OF LINEARLY VARYING STRENGTHS		5. TYPE OF REPORT & PERIOD COVERED Master's and Engineer's degree Thesis June 77
		6. PERFORMING ORG. REPORT NUMBER
7. AUTHOR(s) Bruce Arnold Williams Lt., USN		8. CONTRACT OR GRANT NUMBER(s)
9. PERFORMING ORGANIZATION NAME AND ADDRESS Naval Postgraduate School Monterey, California 93940		10. PROGRAM ELEMENT, PROJECT, TASK AREA & WORK UNIT NUMBERS
11. CONTROLLING OFFICE NAME AND ADDRESS Naval Postgraduate School Monterey, California 93940		12. REPORT DATE June 1977
		13. NUMBER OF PAGES 72
14. MONITORING AGENCY NAME & ADDRESS(if different from Controlling Office) Naval Postgraduate School Monterey, California 93940		15. SECURITY CLASS. (of this report) Unclassified
		15a. DECLASSIFICATION/DOWNGRADING SCHEDULE

16. DISTRIBUTION STATEMENT (of this Report)

Approved for public release; distribution unlimited

17. DISTRIBUTION STATEMENT (of the abstract entered in Block 20, if different from Report)

18. SUPPLEMENTARY NOTES

19. KEY WORDS (Continue on reverse side if necessary and identify by block number)

Potential Flow; Wave Interaction; Green's Function; Source Distribution; Floating Body

20. ABSTRACT (Continue on reverse side if necessary and identify by block number)

Various computer-oriented numerical schemes are available to evaluate the velocity potentials for inviscid fluid flow past submerged objects. The use of a surface distribution of sources of uniform strength over panels representing the object's surface requires a relatively fine grid to obtain accurate results. A new variation of this scheme using distributed sources of linearly varying strengths over triangular panels appears to reduce the number of panels needed for good

DD $_{1 \text{ JAN } 73}^{\text{FORM}}$ 1473   EDITION OF 1 NOV 65 IS OBSOLETE
S/N 0102-014-6601 |

Block 20 con'd

results, thereby reducing computer time and storage require-
ments. In the present study, this technique is applied to
the problem of determining fluid forces and dynamic response
from interaction between an arbitrarily shaped object and
surface waves.

ANALYSIS OF WAVE/OBJECT INTERACTION USING DISTRIBUTED
SOURCE ELEMENTS OF LINEARLY VARYING STRENGTHS

by

Bruce A. Williams
Lieutenant, United States Navy
Bachelor of Science in Electrical Engineering

Submitted in partial fulfillment of the
requirements for the degrees of

MASTER OF SCIENCE IN MECHANICAL ENGINEERING

and

MECHANICAL ENGINEER

from the

NAVAL POSTGRADUATE SCHOOL

June 1977

ABSTRACT

Various computer-oriented numerical schemes are
available to evaluate the velocity potentials for
inviscid fluid flow past submerged objects. The use of
a surface distribution of sources of uniform strength
over panels representing the object's surface requires
a relatively fine grid to obtain accurate results. A
new variation of this scheme using distributed sources
of linearly varying strengths over triangular panels
appears to reduce the number of panels needed for good
results, thereby reducing computer time and storage
requirements. In the present study, this technique is
applied to the problem of determining fluid forces and
dynamic response resulting from interaction between an
arbitrarily shaped object and surface waves.

TABLE OF CONTENTS

5

LIST OF FIGURES

I. INTRODUCTION

Ocean waves interacting with large marine structures produce substantial hydrodynamic forces. These forces are experienced by floating objects such as ships or moored platforms as well as submerged bodies near the free surface, such as submarines at periscope depth or bottom mounted caissons in shallow water.

It is desirable from an engineering standpoint to be able to determine the wave forces and resulting dynamic response for any large ocean structure under design. Until recently, however, such determinations were not possible in the general case. Application of the well-known Morison equation to calculate wave forces is limited to cases in which structure dimensions are small compared to wave length, as in the case of a small diameter pile.

The usual analytical approach in dealing with the hydrodynamic interaction of large bodies with waves is based on a mathematical modeling of the fluid flow using potential flow theory, which assumes the fluid to be inviscid and irrotational. While such an assumption is unrealistic for steady flow past bluff bodies (because of boundary layer separation effects), experiments indicate that it yields valid results for the case of unsteady flow past an object as produced by surface waves provided wave amplitude is small compared to the characteristic dimensions of the object.

Numerical schemes based on the use of the Green's function (or source distribution) method which utilize

7

high-speed computer capabilities have had considerable success in solving problems of wave/body interactions. Garrison, et. al. [Refs. 1-5] have developed numerical procedures for calculation of wave interaction with large, three-dimensional, fixed and floating bodies. These procedures, which represent the immersed surface by a grid of distributed source panels of uniform strengths, have proven to be powerful in practical application as demonstrated in Refs. 6-9.

The most severe limitation of the above mentioned procedures is the rather large amount of computer (C.P.U.) time required to obtain an accurate solution . Thus, any improvements to the method which would improve convergence of the solution would be of considerable value.

A natural extension of the technique based on a uniform distribution of sources over each grid panel is to allow the source strength to vary linearly over the extent of each panel. Since this is not convenient when using quadrilateral panels, it is appropriate to divide the source surface into a grid of triangular panels. The linearly varying source strength may then be represented in terms of the values of the source strength at the corners of the triangles.

Webster [Ref. 10] has developed such a scheme for the case of uniform flow of an unbounded fluid past a three-dimensional body. The body was represented by use of the three-dimensional source potential of the form 1/R where R denotes the distance from the source. In the present study this general method is extended to the problem of representing a body of arbitrary shape located in fluid of finite depth in the presence of a free surface.

The basic approach used in solving the problem of wave interaction with large floating objects is to decompose it into component parts which are more simply analyzed, and then superimpose the results to yield the overall solution. A group of boundary-value problems are generated in terms of velocity potential; one problem is solved for each of the six possible degrees of freedom of body motion, and one for the scattering of the incident wave by the body. The solutions are then formulated in terms of the Green's function. The resulting integral equation is then converted to a system of linear equations which are subsequently solved by computer.

II. FORMULATION OF THE WAVE INTERACTION PROBLEM

A. RESTRICTIONS AND ASSUMPTIONS

All of the usual simplifying assumptions incorporated in
linear gravity wave theory are adopted in the present study.
In summary, these are:

- The flow is considered to be incompressible,
irrotational, and inviscid.
- The wave amplitude to wave length ratio is
small.
- The pressure is uniform above the free surface,
and the density is uniform throughout the fluid.
- The bottom boundary is represented by a
horizontal, impermeable plane.
- The velocity-squared term in Bernoulli's
equation is neglected.
- The waves are regular and periodic.

In addition, it is assumed that

- The object has a smooth, rigid, and impermeable
surface.
- The wave amplitude is small compared to the
object's dimensions.

B. PROBLEM DESCRIPTION

The general description of the problem is shown in Fig.

1, in which two coordinate systems are defined. The inertial coordinate system, positioned at the mean free surface, has directions defined by x, y and z, while the coordinate system positioned on the object has directions indicated by x', y' and z'. The origin of the body coordinates is taken to be at the center of gravity of the body, and the body is submerged an arbitrary distance, d, below the mean free surface. The incident wave is assumed to propagate in the direction defined by the angle γ indicated in Fig. 1.

The analysis of the floating object located in a train of regular waves is decomposed into seven problems which are uncoupled and can be solved independently and superimposed to obtain the complete solution.

The first six problems are identical in form, and consist of determining the fluid forces due to oscillation of the object in the six degrees of freedom, in an otherwise still fluid. The six modes of oscillation are all considered to take place with angular frequency, $\sigma = 2\pi/T$, which matches the frequency of the incident waves. These harmonic motions of the object may be expressed as

$$X_k = Re \left[X_k^o \, e^{-i\sigma t} \right] \qquad , \quad k = 1, 2, \dots, 6 \qquad (1)$$

in which $X_k^o = a\,\Theta_k^o$ when k=4, 5, 6, and where Θ_k^o denotes the angular displacement about the x', y' and z' axes, respectively. The subscripts k=1, 2, 3 correspond to surge, heave, and sway modes of motion, respectively, while the subscripts k=4, 5, 6 correspond to the rotational modes of roll, yaw, and pitch, respectively, as depicted in Fig. 2. The parameter X_k^o denotes the complex amplitude of the linear

11

modes of motion, while the term $a\Theta_k^o$ denotes the complex amplitude of the rotational degrees of freedom.

The seventh problem to be considered is the interaction of waves with the object held fixed in position. This interaction cf an incident wave with the fixed body results in "scattered" waves which radiate from the body. From the solution of this problem the excitation forces and moments acting on the body are determined.

C. EQUATIONS OF MOTION

For a floating body with linear elastic constraints the equation of motion for the six degrees of freedom is given in Ref. 1 as

$$\sum_{j=1}^{6} \left[-\nu(m_{ij}+M_{ij})-i\nu N_{ij}+(K'_{ij}+K_{ij})\right]\frac{X_j^o}{\eta^o} = \left[C_i\right]e^{i\delta t} \qquad (2)$$
$$i=1,2\ldots6$$

where $\nu=\sigma^2/g$, and $\sigma=2\pi/\tau$ denotes the frequency of the incident wave and resulting motion. (In Eq. 2 and all equations which follow, the use of the lower case letter, i, as a subscript denotes an index. Appearance of i elsewhere in an equation denotes the imaginary number $i=\sqrt{-1}$.) The surface elevation of the incident wave at the origin is given by

$$\eta = \eta^o \cos(\sigma t) \qquad (3)$$

in which η^o is a real number denoting the half-amplitude of

12

the incident wave. All phase angles are referred to the wave crest with positive values indicating lag.

In Eq. 2, m_{ij} denotes the dimensionless body mass tensor and is defined by

$$m_{11} = m_{22} = m_{33} = m/\rho a^3 \tag{4a}$$

$$m_{12} = m_{21} = m_{13} = m_{31} = m_{23} = m_{32} = 0 \tag{4b}$$

in which m denotes the mass of the body, ρ denotes the fluid density and a denotes the characteristic length scale of the body. Similarly,

$$m_{44} = I_{44}/\rho a^5, \quad m_{55} = I_{55}/\rho a^5, \quad m_{66} = I_{66}/\rho a^5 \tag{4c}$$

$$m_{45} = m_{54} = -I_{45}/\rho a^5, \quad m_{46} = m_{64} = -I_{46}/\rho a^5 \tag{4d}$$

$$m_{56} = m_{65} = -I_{56}/\rho a^5 \tag{4e}$$

where the moments of inertia are defined typically as

$$I_{45} = I_{54} = \int_m x'y' dm \tag{5a}$$

$$I_{56} = I_{65} = \int_m y'z' dm \tag{5b}$$

in which the integration extends over the complete mass of the body denoted by m.

The excitation force and moment coefficients are defined

as

$$C_j = \frac{F_j(max)\, e^{i\delta_j}}{\rho g\, a^3\, \eta^\circ} \quad , \quad j = 1, 2, 3 \tag{6}$$

$$C_j = \frac{F_j(max)\, e^{i\delta_j}}{\rho g\, a^4\, \eta^\circ} \quad , \quad j = 4, 5, 6 \tag{7}$$

where δ_j denotes the phase shift of the force with respect to the crest of the incident wave. A positive value of δ_j denotes a lag. The term $F_j(max)$, $(j=1, 2, \ldots 6)$, denotes the maximum value of the force $(j=1, 2, 3)$ and moment $(j=4, 5, 6)$ acting on the body.

In the case of the forces (and moments) due to the motion of the body, it is more common to describe the hydrodynamic force in terms of the added mass tensor, M_{ij} and damping tensor N_{ij}. These parameters are defined as

$$-M_{ij} - i\, N_{ij} = \frac{F_{ij}(max)}{\rho \sigma^2\, a^3\, X_j^\circ}\, e^{i\delta_{ij}} \qquad i=1,2,3;\ j=1,2\ldots 6 \tag{8}$$

$$-M_{ij} - i\, N_{ij} = \frac{F_{ij}(max)}{\rho \sigma^2\, a^4\, X_j^\circ}\, e^{i\delta_{ij}} \qquad i=4,5,6;\ j=1,2\ldots 6 \tag{9}$$

where $F_{ij}(max)$ denotes the amplitude of the force or moment in the i-th direction resulting from the motion of the floating body in the j-th degree of freedom.

The forces defined in Eqs. 6-9 are given in terms of surface integrals of the hydrodynamic pressure as

$$F_{ij}(t) = -\iint_S P_j\, h_i\, ds \quad , \quad i, j = 1, 2, \ldots 6 \tag{10}$$

14

$$F_i(t) = - \iint_S P_{07} \, h_i \, ds \qquad , \quad i = 1, 2 \ldots 6 \qquad (11)$$

where F_i denotes the i-th component of wave excitation force or moment and F_{ij} denotes the i-th component of force or moment arising from the j-th component of body motion. The functions h_i are defined as

$$h_1 = n_x \qquad (12a)$$

$$h_2 = n_y \qquad (12b)$$

$$h_3 = n_z \qquad (12c)$$

$$h_4 = (d+y) n_z - z n_y \qquad (12d)$$

$$h_5 = z n_x - x n_z \qquad (12e)$$

$$h_6 = x n_y - (d+y) n_x \qquad (12f)$$

in which n_x, n_y and n_z denote the three components of the outward unit normal vector on the surface of the body.

The parameters P_j, (j=1, 2, ...6), denote the pressure on the immersed surface associated with motion in the six degrees of freedom and P_{07} denotes the pressure associated

15

with the incident wave (0) and scattering (7) of the incident wave. Finally, in Eq. 2 the dimensionless coefficients K_{ij} denote the hydrostatic restoration force (or moment) tensor and are defined as

$$K_{22} = -\frac{1}{a^2} \iint_S n_y \, ds = A_w/a^2 \tag{13a}$$

$$K_{24} = K_{42} = \frac{1}{a^3} \iint_S z' n_y \, ds \tag{13b}$$

$$K_{44} = \frac{1}{a^4} \iint_S (y'z'n_z - z'^2 n_y) ds \tag{13c}$$

$$K_{46} = K_{64} = \frac{1}{a^4} \iint_S x'z' n_y \, ds \tag{13d}$$

$$K_{26} = K_{62} = -\frac{1}{a^3} \iint_S x' n_y \, ds \tag{13e}$$

$$K_{66} = \frac{1}{a^4} \iint_S (x'y' n_x - x'^2 n_y) ds \tag{13f}$$

where A_w denotes the waterline area.

Mooring line reactions depend, in general, on the mooring line configuration, weight, shape (catenary), hydrodynamic and elastic properties. However, it is generally permissible to disregard dynamic effects and approximate the reactions by a linear relationship with the six components of body displacements as indicated by Eq. 2. The term K'_{ij} in Eq. 2 represents the dimensionless force (or moment) produced in the (negative) i-direction by a unit

displacement of the body in the j-direction. Given the mooring line configuration and elastic properties, the

16

spring constant tensor can be evaluated.

D. REPRESENTATION BY VELOCITY POTENTIALS

The fluid motion in each of the seven flow situations previously described can be represented by a velocity potential. Specification of the velocity potential of a flow completely describes the flow, since fluid velocities at any point are obtainable through the relation

$$\bar{q}(x,y,z,t) = \nabla \bar{\Phi}(x,y,z,t) \tag{14}$$

where $\bar{q}(x,y,z,t)$ represents the velocity vector, $\bar{\Phi}(x,y,z,t)$ represents the time dependent velocity potential, and $\nabla \bar{\Phi}$ denotes the gradient of the potential. Thus, for the six modes of oscillation of the body in still water, the fluid velocity vector is given by

$$\bar{q}_k(x,y,z,t) = \nabla \bar{\Phi}(x,y,z,t) = Re\left[\nabla \phi_k(x,y,z)e^{-i\sigma t}\right] \tag{15}$$
$$k = 1,2\ldots 6$$

in which $\phi_k(x,y,z)$ denotes the complex space dependent part of the total potential induced by the k-th mode of oscillation. The velocity potential associated with the seventh problem, waves interacting with the fixed body, is actually composed of two components. One component is the potential due to the linear incident wave, the space dependent part of which is given by

$$\Phi_0 = -\frac{ig\eta^\circ}{\sigma}\left(\frac{\cosh k(h+y)}{\cosh kh}\right)e^{i[kx\cos\gamma + kz\sin\gamma]} \tag{16}$$

17

in which η^o=H/2 denotes wave amplitude (half-amplitude) and
k= 2π/L denotes wave number.

The seccnd component of the wave interaction potential
is due to the presence of waves whose characteristics have
been altered by interacting with the object. This potential
is referred to as the scattering potential and is denoted by
the subscript (7). The total potential for the motion of the
body in regular waves is expressed through the superposition

$$\Phi(x,y,z,t) = \sum_{k=0}^{7} \Phi_k(x,y,z,t) \tag{17}$$

E. THE ECUNDARY-VALUE PROBLEM

Each of the velocity potentials (ϕ_k, k=1,2...7) must
satisfy the continuity equation, which in the case of
irrotaticnal flow takes the form

$$\nabla^2 \phi_k(x,y,z) = 0 \quad , \quad k = 0,1...7 \tag{18}$$

In addition, the pctentials must also satisfy the kinematic
bottom bcundary condition

$$\frac{\partial \phi_k}{\partial y}(x,-h,z) = 0 \quad , \quad k = 0,1...7 \tag{19}$$

where h denotes the mean water depth, as well as the
linearized dynamic and kinematic free surface boundary
conditions expressed by

18

$$\frac{\partial \phi_k}{\partial y}(x,0,z) - \frac{\sigma^2}{g} \phi_k(x,0,z) = 0 \quad , \quad k = 0,1,\dots 7 \tag{20}$$

where g denotes the acceleration of gravity.

While the free surface and bottom boundary conditions are exactly the same for all of the potentials, the kinematic boundary condition applied on the surface of the object is different for each case. This boundary condition results from the assumption that the surface of the object is rigid and impermeable; it simply imposes the condition that there be no normal component of fluid velocity relative to the surface at any point on the surface, and is expressed mathematically as follows:

For oscillation of the body in the still fluid,

$$\frac{\partial \phi_1}{\partial n} = g_1 = -i\sigma X_1^0 n_x \tag{21a}$$

$$\frac{\partial \phi_2}{\partial n} = g_2 = -i\sigma X_2^0 n_y \tag{21b}$$

$$\frac{\partial \phi_3}{\partial n} = g_3 = -i\sigma X_3^0 n_z \tag{21c}$$

$$\frac{\partial \phi_4}{\partial n} = g_4 = -i\sigma \Theta_4^0 [(d+y)n_z + zn_y] \tag{21d}$$

$$\frac{\partial \phi_5}{\partial n} = g_5 = -i\sigma \Theta_5^0 [zn_x - xn_z] \tag{21e}$$

$$\frac{\partial \phi_6}{\partial n} = g_6 = -i\sigma \Theta_6^0 [xn_y - (d+y)n_x] \tag{21f}$$

where n_x, n_y and n_z denote the x, y and z components of the unit outward normal vector on the immersed surface which is

defined in its mean position by $S(x,y,z)=0$.

For wave interaction with the fixed body,

$$\frac{\partial \Phi_7}{\partial n} = g_7 = \frac{-\partial \Phi_o}{\partial n} = \frac{ig\eta^o k}{\sigma \cosh(kh)} e^{i(kx\cos\gamma + kz\sin\gamma)}$$

$$\cdot \left[n_y \sinh[k(h+y)] + i(n_x\cos\gamma + n_z\sin\gamma) \cdot \cosh[k(h+y)]\right] \qquad (22)$$

in which γ denotes the angle between the incident wave propagation direction and the x'-axis. Equations 21 and 22 are applied only on the immersed surface as defined by $S(x,y,z)=0$.

III. SOLUTION OF THE BOUNDARY-VALUE PROBLEM

A. GREEN'S FUNCTION SOLUTION

In using Green's function representation of the velocity
potential, each of the seven unknown potentials is
considered to be induced by fluid sources which are
distributed over the surface of the body in a continuous
manner. The strength of the source at any location on the
body surface is a function of position and is denoted by
$f(\xi,\eta,\zeta)$, where (ξ,η,ζ) indicates a point on the immersed
surface. (Figure 3 illustrates the concept of the continuous
source distribution.) The velocity potential associated with
each of the boundary value problems is then given by the
surface integral

$$\phi_k(x,y,z) = \iint_S f_k(\xi,\eta,\zeta)\, G(x,y,z;\xi,\eta,\zeta)\, ds \qquad (23)$$
$$k = 1,2\ldots,7$$

where $G(x,y,z;\xi,\eta,\zeta)$ is referred to as the Green's
function. Its value depends upon the location of the point
(ξ,η,ζ) on the source surface, and the point (x,y,z) in the
fluid field. The Green's function for the present case,
which satisfies the bottom and free surface boundary
conditions, is given by

$$G = \frac{1}{R} + \frac{1}{R'} + G^* \qquad (24)$$

in which

$$R = \sqrt{(\xi - x)^2 + (\eta - y)^2 + (\zeta - z)^2} \qquad (25a)$$

$$R' = \sqrt{(\xi - x)^2 + (y + 2h + \eta)^2 + (\zeta - z)^2} \qquad (25b)$$

The G* term is given by Ref. 3 as

$$G^*(x,y,z;\xi,\eta,\zeta) = 2 \; P.V. \int_0^\infty$$

$$\frac{(\mu + \nu) e^{-\mu h} \cosh[\mu(\eta + h)] \cosh[\mu(y + h)] J_0(\mu r) d\mu}{\mu \sinh(\mu h) - \nu \cosh(\mu h)}$$

$$+ \frac{i 2\pi (k^2 - \nu^2) \cosh[k(\eta + h)] \cosh[k(y + h)] J_0(kr)}{k^2 h - \nu^2 h + \nu} \qquad (26)$$

in which

$$r = \sqrt{(x - \xi)^2 + (z - \zeta)^2} \qquad (27)$$

The term J_0 denotes the Bessel function of the first kind, of order zero, and ν represents dimensionless wave frequency. P.V. indicates the principal value of the infinite integral.

An alternate series form of the complete Green's function is given by

$$G = \frac{2\pi(\nu^2 - k^2)}{k^2 h - \nu^2 h + \nu} \cosh[k(h + \eta)] \cosh[k(y + h)][Y_0(kr) - i J_0(kr)]$$

$$+4\sum_{k=1}^{\infty}\frac{(\mu_k^2+\nu^2)}{\mu_k^2 h+\nu^2 h-\nu}\cos[\mu_k(y+h)]\cos[\mu_k(\eta+h)]K_0(\mu_k r) \qquad (28)$$

in which Y_0 denotes the Bessel function of the second kind, of order zero, K_0 denotes the modified Bessel function of the second kind, of order zero, and μ_k represents the real positive roots of the equation

$$\mu_k\ tan\ (\mu_k h)+\nu=0 \qquad (29)$$

In numerical evaluations either form of the Green's function may be used with the exception of the case where r approaches zero. Here the series form given in Eq. 28 is singular so the integral form given by Eq. 26, which has a well-defined 1/R singularity, is used. However, when r is not small the series form is generally used for numerical calculation because it requires less computer time for evaluation.

The Green's function representation of the potential given by Eq. 24 satisfies the laplace equation as well as the free surface and bottom boundary conditons for all cases. The source strength function $f_k(\xi,\eta,\zeta)$ is unknown and is determined by application of the kinematic boundary conditions on the body surface (Eqs. 21 and 22). This results in the following integral equation:

$$\frac{1}{4\pi}\iint_S f_k\ (\xi,\eta,\zeta)\frac{\partial G}{\partial n}\ (\xi,\eta,\zeta;x,y,z)\,ds = g_k(x,y,z) \qquad (30)$$
$$k=1,2\ldots7$$

in which $\partial G/\partial n$ denotes the deriviative of the Green's function in the outward normal direction, which is given by

$$\frac{\partial G}{\partial n}(x,y,z\,;\,\xi,\eta,\varsigma) = \nabla G(x,y,z\,;\,\xi,\eta,\varsigma)\cdot\bar{n} \qquad (30a)$$

where $\bar{n}$ represents the outward unit normal vector at (x,y,z) and where (x,y,z) now represents a control point on $S(x,y,z)=0$.

For the seven problems, all quantities in Eq. 30 are known except for the source strength functions $f_k(\xi,\eta,\varsigma)$, $(k=1,2,\ldots7)$. However, the integral equation cannot be solved analytically for an arbitrarily shaped body, and a numerical approach must be adopted. The numerical approach developed herein involves discretizing both the source strength function and the body surface boundary condition functions, g_k, $(k=1,2,\ldots7)$.

B. DISCRETIZATION OF THE PROBLEM

1. Uniform Source Strength Element Method

The technique previously used [Ref. 1] to discretize the integral equations given by Eq. 30 is to divide the source distribution into a grid of N quadrilateral panels, and to assume that the source strength has a distinct, constant value over each panel. Hence, for any of the seven flow problems of interest here, f_{k_j} denotes the strength of the source everywhere on panel j, $(j=1,2\ldots N)$, for the k-th problem $(k=1,2\ldots7)$. The area of panel j is denoted by ΔS_j and the induced potential anywhere in the fluid thus results from a summation of the effects of all the source

24

panels. Figure 4 depicts the discretized source surface and
resulting potential.

Additionally, the normal boundary condition
functions $g_k(x,y,z)$, $(k=1,2...7)$, of Eq. 30 are discretized
by applying the kinematic body surface boundary condition at
only M selected points on the surface. In practice, the
number of boundary condition ("control") points are chosen
to be equal $(M=N)$. For convenience, the control points are
chosen to lie at the centroids of the source panels. Thus,
for each discretized integral equation, a system of N linear
equations in N unknowns results:

$$\frac{1}{4\pi} \sum_{j=1}^{N} f_{k_j} \iint_{\Delta s_j} \frac{\partial G}{\partial n}(x_i, y_i, z_i; \xi, \eta, \zeta)\, ds = g_{k_i} \qquad \begin{array}{l} k=1,2...7 \\ i=1,2...N \end{array} \qquad (31)$$

in which (x_i, y_i, z_i) represents a control point i on the body
surface, at which the boundary condition is being applied,
and g_{k_i} denotes the value of $g_k(x,y,z)$ at point i.   Equation
31 is expressed in matrix form as

$$[\alpha] \left\{ f_k \right\} = \left\{ g_k \right\} \qquad k=1,2...7 \qquad (32)$$

where $[\alpha]$ is an NxN matrix composed of elements

$$\alpha_{ij} = \sum_{j=1}^{N} \iint_{\Delta s_j} \frac{\partial G}{\partial n}(x_i, y_i, z_i; \xi, \eta, \zeta)\, ds \qquad (33)$$

The vectors $\left\{ f_k \right\}$ and $\left\{ g_k \right\}$ represent the N unknown source
strengths and the kinematic boundary condition applied at
the N control points, respectively, for the k-th flow

25

problem. It should be noted that the matrix $[\alpha]$ depends only on the body configuration, water depth, and period of the motion and is the same for all seven cases.

The discretized potential which is induced by the N source panels is specified by a matrix equation similar to Eq. 20:

$$\left\{ \phi_k \right\} = \left[\beta \right] \left\{ f_k \right\} \qquad k = 1, 2 \ldots 7 \qquad (34)$$

The martix $[\beta]$ is composed of elements

$$\beta_{ij} = \frac{1}{4\pi} \sum_{j=1}^{N} \iint_{\Delta S_j} G(\xi, \eta, \zeta; x_i, y_i, z_i) \, ds \qquad (35)$$

As in the case of matrix $[\alpha]$, matrix $[\beta]$ is the same for all seven flcw cases.

Integration of the Green's function and its derivatives in Eqs. 33 and 35 poses no great difficulty. It is most convenient to separately integrate the singular terms. Special considerations in performing these integrations and necessary formulas are provided in Ref. 2.

A ccmputer solution of Eq. 32 is accomplished using matrix inversicn and multiplication, yielding the previously unknown values of the source strengths. Values of velocity potential at the control points (panel centroids) are then obtained directly using Eqs. 34 and 35. Fluid velocities at the contrcl points are similarly obtained after first differentiating the elements of the $[\beta]$ matrix with respect to the x,y and z directions. Dynamic pressures are calculated frcm the linearized form of Bernoulli's equation. Finally, the forces acting on the object are determined by pressure integraticn (or more precisely, summation) over the

26

surface area of the object as indicated by Eqs. 10 and 11.

2. Method of Linearly Varying Source Strength Elements

An alternative method of discretizing the Green's function integral equations, proposed by Webster [Ref. 10] for uniform unbounded flow past a submerged body, utilizes triangular source panels over which the source strength function is considered to vary linearly. In this way, the discontinuities or "jumps" in source strengths at adjoining panel edges (which existed in the previous scheme) are eliminated. Also, since source strengths are not held constant over the extent of each panel, the discretization results in a less crude approximation of the continuous strength function. An additional "smoothing" effect on the velocities induced near the body is achieved by submerging the source panel surface inward a selected distance from the actual body surface, although the kinematic body boundary condition is still applied at points on the true body surface. It is noted that while some smoothing effect can be accomplished by submerging the sources, this is not a necessity as long as the singularity is accounted for properly.

Figure 5 depicts the linearly varying source strength function for a single triangular panel. The local coordinate system for each panel is defined such that two triangle corners (denoted by a and d) lie on the local x-axis, and the third corner (b) lies on the positive y-axis. Appendix A gives the transformation between the body coordinate system and the local coordinate system for a given panel.

In panel coordinates, the linearly varying source strength function may be written

27

$$f(\tilde{\xi}, \tilde{\eta}) = \alpha + \beta \tilde{\xi} + \gamma \tilde{\eta} \tag{36}$$

in which α, β and γ denote constant coefficients and the tildes indicate local coordinate values as defined in Fig. 5. The values of the source strength at the three corners are

$$f_a \equiv f(a, 0) \tag{37a}$$

$$f_b \equiv f(0, b) \tag{37b}$$

$$f_d \equiv f(d, 0) \tag{37c}$$

Substitutuion of Eqs. 37 into Eq. 36 allows the constant coefficients to be expressed in terms of the triangle geometry and the values of the strength at the corners:

$$\beta = (f_a - f_d)/(a - d) \tag{38a}$$

$$\alpha = (a f_d - d f_a)/(a - d) \tag{38b}$$

$$\gamma = [(a - d) f_b - a f_d + d f_a]/b(a - d) \tag{38c}$$

Thus, the contribution to the potential at (x, y, z) due to the single panel of area ΔS is denoted by $\Delta \phi(x, y, z)$ and is given by:

$$\Delta\phi(\tilde{x},\tilde{y},\tilde{z}) = \frac{1}{4\pi} \iint_{\Delta S} (\alpha + \beta\,\tilde{\xi} + \gamma\tilde{\eta})\, G(\tilde{\xi},\tilde{\eta};\tilde{x},\tilde{y},\tilde{z})\, ds \tag{39}$$

where $\tilde{\xi}$ and $\tilde{\eta}$ denote local panel coordinates and (x,y,z) denotes a general point expressed in terms of local coordinates.

Substituting Eqs. 38 into Eq. 39 and collecting terms allows the contribution to the potential to be expressed in terms of the values of the source strength at the corners of the panel:

$$\Delta\phi(\tilde{x},\tilde{y},\tilde{z}) = f_a\,\Delta\phi_a + f_b\,\Delta\phi_b + f_d\,\Delta\phi_d \tag{40}$$

in which

$$\Delta\phi_a = \iint_{\Delta S} \frac{-bd + b\,\tilde{\xi} + d\,\tilde{\eta}}{4\pi\, b(a-d)}\, G(\tilde{\xi},\tilde{\eta};\tilde{x},\tilde{y},\tilde{z})\, ds \tag{41a}$$

$$\Delta\phi_b = \iint_{\Delta S} \frac{\tilde{\eta}}{4\pi b}\, G(\tilde{\xi},\tilde{\eta};\tilde{x},\tilde{y},\tilde{z})\, ds \tag{41b}$$

$$\Delta\phi_d = \iint_{\Delta S} \frac{ab - b\,\tilde{\xi} - a\,\tilde{\eta}}{4\pi\, b(a-d)}\, G(\tilde{\xi},\tilde{\eta};\tilde{x},\tilde{y},\tilde{z})\, ds \tag{41c}$$

For convenience $\Delta\phi_a$, $\Delta\phi_b$ and $\Delta\phi_d$ will be referred to as simply the "corner integrals" associated with corners a,b and d, respectively, for a given triangular panel.

The velocity induced by a single source panel is obtained by taking the gradient of Eq. 40:

$$\Delta\bar{q}(\tilde{x},\tilde{y},\tilde{z}) = f_a\nabla(\Delta\phi_a) + f_b\nabla(\Delta\phi_b) + f_d\nabla(\Delta\phi_d) \tag{42}$$

The gradients of the corner integrals are given by

$$\nabla(\Delta\phi_a) = \iint_{\Delta S} \frac{-bd+b\bar{\xi}+d\bar{\eta}}{4\pi \ b(a-d)} \nabla G(\tilde{\xi},\tilde{\eta};\tilde{x},\tilde{y},\tilde{z})\,ds \qquad (43a)$$

$$\nabla(\Delta\phi_b) = \iint_{\Delta S} \frac{\tilde{\eta}}{4\pi b} \nabla G(\tilde{\xi},\tilde{\eta};\tilde{x},\tilde{y},\tilde{z})\,ds \qquad (43b)$$

$$\nabla(\Delta\phi_d) = \iint_{\Delta S} \frac{ba-b\bar{\xi}-a\tilde{\eta}}{4\pi b(a-d)} \nabla G(\tilde{\xi},\tilde{\eta};\tilde{x},\tilde{y},\tilde{z})\,ds \qquad (43c)$$

The evaluation of the three corner integrals (Eq. 41) and their gradients (Eq. 43) must be accomplished in local coordinates for each panel. In performing the integrations, it is most efficient to separate the Green's function into its singular and non-singular components, and treat the integrals separately, as follows:

$$\Delta\phi_a = \iint_{\Delta S} W_a \ (1/R)ds + \iint_{\Delta S} W_a \ (1/R')ds + \iint_{\Delta S} W_a \ (G^*)\,ds \qquad (44a)$$

$$\Delta\phi_b = \iint_{\Delta S} W_b \ (1/R)ds + \iint_{\Delta S} W_b \ (1/R')ds + \iint_{\Delta S} W_b \ (G^*)\,ds \qquad (44b)$$

$$\Delta\phi_d = \iint_{\Delta S} W_d \ (1/R)ds + \iint_{\Delta S} W_d \ (1/R')ds + \iint_{\Delta S} W_d \ (G^*)\,ds \qquad (44c)$$

$$\nabla(\Delta\phi_a) = \iint_{\Delta S} W_a \nabla(1/R)\,ds + \iint_{\Delta S} W_a \nabla(1/R')\,ds + \iint_{\Delta S} W_a \nabla(G^*)\,ds \qquad (45a)$$

$$\nabla(\Delta\phi_b) = \iint_{\Delta S} W_b \nabla(1/R)\,ds + \iint_{\Delta S} W_b \nabla(1/R')\,ds + \iint_{\Delta S} W_b \nabla(G^*)\,ds \qquad (45b)$$

$$\nabla(\Delta\phi_d) = \iint_{\Delta S} W_d \nabla(1/R)\,ds + \iint_{\Delta S} W_d \nabla(1/R')\,ds + \iint_{\Delta S} W_d \nabla(G^*)\,ds \qquad (45c)$$

in which W_a, W_b, and W_d are linear functions in $\tilde{\xi}$ and $\tilde{\eta}$ and are given by

$$W_a = -\frac{bd + b\tilde{\xi} + d\tilde{\eta}}{4\pi b(a-d)} \tag{46a}$$

$$W_b = \frac{\eta}{4\pi b} \tag{46b}$$

$$W_d = \frac{ba - b\tilde{\xi} - a\tilde{\eta}}{4\pi b(a-d)} \tag{46c}$$

Appendix B provides formulas developed by Webster [Ref. 10] for the closed form evaluation of those integrals in Eqs. 44 and 45 which involve derivatives of 1/R and 1/R' as well as similar formulas developed by Yeung and Bai [Ref. 11] for integrals of 1/R and 1/R'. The integrands are singular, and it is therefore necessary to evaluate the integrals analytically.

Integration of the G* components of Eqs. 44 and 45 is made possible by assuming that the G* function and its gradient vary linearly over the triangular panel, (as was done for the source strength function). This is a reasonable approximation since G* is a well-behaved function that varies slowly with position on the body surface. The wave length of its oscillation is approximately the same as the wave length of the incident wave, and this tends to be large relative to the panel dimensions in typical applications.

With G* and ∇ G* expressed as linear functions of their values at the panel corners, the terms in Eqs. 44 and 45 involving these two functions may be expressed as

31

$$\iint_{\Delta s} W_a \, G^* \, ds \;=\; I_a \left(a, b, d, \, G_a^*, \, G_b^*, \, G_d^*\right) \tag{47a}$$

$$\iint_{\Delta s} W_b \, G^* \, ds \;=\; I_b \left(a, b, d, \, G_a^*, \, G_b^*, \, G_d^*\right) \tag{47b}$$

$$\iint_{\Delta s} W_d \, G^* \, ds \;=\; I_d \left(a, b, d, \, G_a^*, \, G_b^*, \, G_d^*\right) \tag{47c}$$

$$\iint_{\Delta s} W_a \, \nabla G^* \, ds \;=\; I_a' \left(a, b, d, \, \nabla G_a^*, \, \nabla G_b^*, \, \nabla G_d^*\right) \tag{48a}$$

$$\iint_{\Delta s} W_b \, \nabla G^* \, ds \;=\; I_b' \left(a, b, d, \, \nabla G_a^*, \, \nabla G_b^*, \, \nabla G_d^*\right) \tag{48b}$$

$$\iint_{\Delta s} W_d \, \nabla G^* \, ds \;=\; I_d' \left(a, b, d, \, \nabla G_a^*, \, \nabla G_b^*, \, \nabla G_d^*\right) \tag{48c}$$

where I_a, I_b, I_d, I_a', I_b', I_d', represent the integrals of the product of the two linear functions over the triangular area. The integrals in Eqs. 47 and 48 were evaluated using the formulas given in appendix C for integrating the product of two linear functions over a triangular area and the resulting integrals are given in Appendix D

The total potential and velocity at any point in the fluid is a result of the combined effects of all the source panels. For a grid composed of M panels, the potential is given by

$$\Phi(x,y,z) = \sum_{k=1}^{M} f_{a_k} \Delta \phi_{a_k}(x,y,z) + f_{b_k} \Delta \phi_{b_k}(x,y,z) + f_{d_k} \Delta \phi_{d_k}(x,y,z) \tag{49}$$

and the velocity vector is given by

$$\bar{q}(x,y,z) = \sum_{k=1}^{M} f_{a_k} \nabla \left(\Delta \phi_{a_k}(x,y,z)\right) + f_{b_k} \nabla \left(\Delta \phi_{b_k}(x,y,z)\right) + f_{d_k} \nabla \left(\Delta \phi_{d_k}(x,y,z)\right) \tag{50}$$

in which f_{a_k}, f_{b_k}, f_{d_k}, denote the strengths at the three corners of the k-th panel.

It should be emphasized that the corner integrals and their gradients are evaluated in their own individual panel coordinate systems. Transformation back to the global coordinates, described in Appendix A, must be accomplished prior to performing the summations of Eqs. 49 and 50.

The summations given in Eqs. 49 and 50 can be re-arranged by reversing the order of the summation. That is, if coefficients of the strength at a given node are first summed, then the summation may be written

$$\phi(x,y,z) = \sum_{j=1}^{N} f_j \, \Delta\phi_j \, (x,y,z) \tag{51}$$

$$\bar{q}(x,y,z) = \sum_{j=1}^{N} f_j \, \nabla\big(\Delta\phi_j(x,y,z)\big) \tag{52}$$

in which f_j denotes the source strength at corner node j (j=1,2...N) and $\Delta\phi_j$ represents the sum of the corner integrals associated with node j, for all panels which share node j as a mutual corner. A graphic representation of the meaning of $\Delta\phi_j$ is provided in Fig. 6 for clarity, since it is difficult to express mathematically. As indicated in Fig. 6 $\Delta\phi_j(x,y,z)$ denotes the contribution to the potential at (x,y,z) from the panels surrounding node j.

Each of the surrounding panels may be considered to have unit strength at the corner coincident with node j and zero at the other two corners as depicted in Fig. 6.

The kinematic boundary condition at the body surface may now be applied at N selected points. It is convenient to use points on the surface which lie directly outward from the corner nodes of the submerged source surface. In practice, it is best to initially define the nodes on the actual body surface, and then establish the points on the submerged grid at some pre-selected submergence distance along the corresponding inward normal vectors.

Application of the kinematic boundary conditions for each of the seven problems of interest results in the discretized version of the integral equation:

$$f_{k_j} \frac{\partial (\Delta \phi_{i,j})}{\partial n} = g_{k_i} \quad , k = 1, 2 \dots 7; \ i = 1, 2 \dots N \quad (53)$$

where the repeated index j indicates summation. The term denotes the sum of the corner integrals for node j, evaluated at control point i. The derivative with respect to the outward normal vector is obtained by

$$\frac{\partial (\Delta \phi_{i,j})}{\partial n} = \nabla (\Delta \phi_{i,j}) \cdot \bar{n}_i \quad (54)$$

where $\bar{n}_i$ is the unit outward normal vector at the control point i, on the body surface.

Equation 53 may be expressed more simply as

$$[\alpha] \{ f_k \} = \{ g_k \} \quad , k = 1, 2 \dots 7 \quad (55)$$

where the NxN matrix, $[\alpha]$, is composed of elements

34

$$\alpha_{ij} = \frac{1}{4\pi} \frac{\partial(\Delta\phi_{ij})}{\partial n} \tag{56}$$

Equation 55 is solved by computer, (for k=1,2...7) using matrix inversion and multiplication, yielding the unknown source strengths. Substitution of the source strengths into Eqs. 51 and 52 with evaluation at (x_i, y_i, z_i) (i=1,2,...N), gives the values of the potential and the fluid velocities at the control points on the body surface.

The dynamic fluid pressure is determined using the linearized form of Bernoulli's equation. For oscillation of the body in its six degrees of freedom, the pressures at the surface nodes (denoted by i) are given by:

$$P_{k_i} = Re\left[i\rho\sigma\,\phi_{k_i}e^{-i\sigma t}\right] \qquad , \quad k = 1, 2 \ldots 7 \tag{57}$$

$$P_{o7_i} = Re\left[i\rho\sigma\,(\phi_{o_i} + \phi_{7_i})e^{-i\sigma t}\right] \tag{58}$$

where ρ denotes fluid density, and P_{k_i} and ϕ_{k_i} denote dynamic pressure and potential, respectively, at node i (denoted by the subscript i) due to motion in the k-th mode of oscillation.

The pressure integrals given by Eqs. 10 and 11 cannot be utilized directly to obtain total forces and moments, because only discrete values of pressures are available. However, it is consistent with the numerical scheme to assume that the pressure varies linearly over each triangular panel. Based on this assumption, the pressure at any point on a surface panel is expressed as a linear function of the panel geometry and the values at the corner

35

nodes, which are given by Eqs. 57 and 58.

The forces and moments are then calculated using

$$F_{ik}(t) = \sum_{i=1}^{M} \iint_{\Delta S_i} P_k \, h_i \, ds \quad , \quad i, k = 1, 2 \ldots 6 \qquad (59)$$

$$F_i(t) = \sum_{i=1}^{M} \iint_{\Delta S_i} P_{07} \, h_i \, ds \quad , \quad i = 1, 2 \ldots 6 \qquad (60)$$

where F_i denotes the i-th component of wave excitation force or moment and F_{ik} denotes the i-th component of force or moment arising from the k-th component of body motion. The summations of Eqs. 59 and 60 are carried out over the M panels on the actual body surface. The functions h_i are given by Eq. 12 and are functions of position on the immersed surface. It appears to be consistent with the numerical scheme to approximate these functions as linear functions so that they may be defined at interior points by their values at the corners of the triangles. Thus the integrands of Eqs. 59 and 60 contain the products of two linear functions. The integrals are evaluated in a straight-forward manner using the integration formulas given in Appendix C .

The resulting forces F_{ik} (i,k=1,2...6) and F_i (i=1,2...6) are substituted into Eqs. 6, 7, 8 and 9 to evaluate the excitation force coefficients C_j (j=1,2,...6), and the added mass and damping coefficients, M_{ij}, and N_{ij}, (i,j=1,2,...6). Finally, the equations of motion for the six degrees of freedom (Eq. 2) are applied to determine the

complete dynamic response of the body.

IV. NUMERICAL RESULTS

A computer code based on the numerical method outlined was developed to calculate the hydrodynamic coefficients as well as the dynamic response of a floating body in waves. Using this program, example calculations were made for two simple geometric shapes: a vertical circular cylinder which extends from the bottom and passes through the free surface, and a semi-immersed sphere. Computer produced drawings of the grid configurations used are shown in Figs. 7-10.

The vertical circular cylinder represents the only three-dimensional geometry for which a closed-form solution exists (of the type of interest in the present study), and therefore, it is of interest for making a comparison of numerical results computed by the present method. MacCamy and Fuchs [Ref. 12] have developed a closed form solution for the horizontal force acting on the cylinder and this result is plotted in in Fig. 11 in the form of the dimensionless amplitude of the force versus the wave length parameter, $2\pi a/L$.

Corresponding results computed by the triangular panel method using grids of two different finenesses are shown on Fig. 11 for comparison with the results of MacCamy and Fuchs. These results indicate rather rapid convergence of the solution, particularily at small values of $2\pi a/L$. The slower convergence (or greater error) at the larger values of $2\pi a/L$ apparently indicates the inaccuracies associated with the assumption of linearly varying source strength. As $2\pi a/L$ becomes large (the wave length becomes small) the variation of the G^* part of the Green's function with

38

distance becomes more rapid. Thus, as $2\pi a/L$ increases, a point is reached where the assumption of the linear variation of the Green's function becomes appreciably invalid. Of course, as the fineness of the grid is increased the numerical results tend to agree with the closed-form exact results up to higher values of $2\pi a/L$.

Havelock [Ref. 13] has presented results for the added mass and damping coefficient in heave for a semi-immersed sphere and these results are presented in Fig. 12 for comparison with numerical results computed by the present method. The figure shows the heave added mass and damping coefficients, M_{22} and N_{22}, respectively, for the semi-immersed sphere along with the numerical results computed using grids of two different finenesses. These results indicate that the numerical results are tending to converge although even for the finer grid the results are not yet converged.

Moreover, given the damping coefficient, the wave force coefficient can be computed by use of the Haskind's relations which, in general, relate the force coefficients to the far-field solutions of the corresponding radiation problem. For the case of the heaving motion of an axi-symmetric body a closed form relationship exists between the heave damping coefficient and heave excitation force. Thus, Havelock's results for the damping coefficient in heave were used to compute the heave excitation force and this result is presented in Fig. 13 for comparison with the numerical results.

The numerical results presented for comparison with Havelock's results in Fig. 13 show a trend toward convergence and, in fact, the results corresonding to the finer grid indicate adequate agreement.

39

Finally, the dynamic response in heave and surge for the case of the semi-immersed sphere are shown in Fig. 14. These results, showing the dimensionless response in terms of the response amplitude to wave amplitude ratio, indicate very little difference between the the two grid finenesses.

V. CONCLUSIONS

A new numerical procedure based on the use of triangular source panels has been developed for computing the interaction of fixed or floating bodies with waves. Numerical results based on this procedure compare well with existing results, and, in general, the procedure appears to converge to the correct solution.

The value of the triangular panel procedure as compared to the procedure based on quadrilateral panels of uniform strength remains uncertain. This will be determined only through experience in application of the two methods.

APPENDIX A

COORDINATE TRANSFORMATION

In the following, the coordinate transformation is
developed which relates the local coordinates attached to a
particular panel, as indicated in figure 1a, to the global
coordinates with origin located at the mean water level. The
global system is denoted by $O(x,y,z)$ and the local
coordinate system is denoted by $O(\tilde{x},\tilde{y},\tilde{z})$.
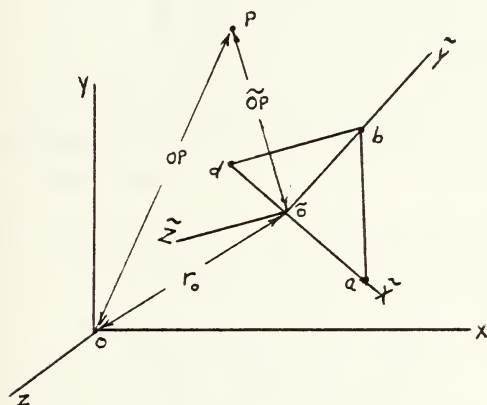
Figure 1a-Coordinate System Locations

The location of the origin of the local coordinate
system expressed in global coordinates is given by

$$\left[X_o, Y_o, Z_o\right] = \left[\left(x_d + \alpha(x_a - x_d)\right), \left(Y_d + \alpha(Y_a - Y_d)\right), \left(Z_d + \alpha(Z_a - Z_d)\right)\right]$$

in which (x_a, y_a, z_a), (x_b, y_b, z_b) and (x_d, y_d, z_d) are the global system coordinates of the triangle corners a, b and d, respectively, and where

$$\alpha = \frac{(x_a - x_d)(x_b - x_d) + (y_a - y_d)(y_b - y_d) + (z_a - z_d)(z_b - z_d)}{(x_a - x_d)^2 + (y_a - y_d)^2 + (z_a - z_d)^2}$$

The unit vectors in the $\tilde{x}, \tilde{y}$ and $\tilde{z}$ directions of the local coordinate system are given in terms of their respective global system components as

$$\bar{\tilde{i}} = u_{x_1}\bar{i} + u_{x_2}\bar{j} + u_{x_3}\bar{k}$$

$$\bar{\tilde{j}} = u_{y_1}\bar{i} + u_{y_2}\bar{j} + u_{y_3}\bar{k}$$

$$\bar{\tilde{k}} = u_{z_1}\bar{i} + u_{z_2}\bar{j} + u_{z_3}\bar{k}$$

in which $\bar{\tilde{i}}$, $\bar{\tilde{j}}$ and $\bar{\tilde{k}}$ are the unit vectors in the $\tilde{x}$, $\tilde{y}$ and $\tilde{z}$ directions, and $\bar{i}$, $\bar{j}$ and $\bar{k}$ are the unit vectors in the x, y and z directions.

The terms u_{x_1}, u_{x_2}, ... u_{z_3} are defined as follows:

$$u_{x_1} = (x_a - x_d)/|\overline{da}|$$

$$u_{x_2} = (y_a - y_d)/|\overline{da}|$$

$$u_{x_3} = (z_a - z_d)/|\overline{da}|$$

$$u_{y_1} = (x_b - x_o)/|\overline{ob}|$$

$$u_{y_2} = (y_b - y_o)/|\overline{ob}|$$

43

$$u_{Y_3} = (z_b - z_o)/|\overline{ob}|$$

$$u_{Z_1} = u_{x_2} u_{Y_3} - u_{x_3} u_{Y_2}$$

$$u_{Z_2} = u_{x_3} u_{Y_1} - u_{x_1} u_{Y_3}$$

$$u_{Z_3} = u_{x_1} u_{Y_2} - u_{x_2} u_{Y_1}$$

where

$$|\overline{da}| = \sqrt{(x_a - x_d)^2 + (y_a - y_d)^2 + (z_a - z_d)^2}$$

and

$$|\overline{ob}| = \sqrt{(x_o - x_b)^2 + (y_o - y_b)^2 + (z_o - z_b)^2}$$

The transformation matrix is then defined as

$$
[T] = \begin{bmatrix} u_{x_1} & u_{x_2} & u_{x_3} \\ u_{Y_1} & u_{Y_2} & u_{Y_3} \\ u_{z_1} & u_{z_2} & u_{z_3} \end{bmatrix}
$$

Transformation between global coordinates and local coordinates is accomplished in the following manner:

$$
\begin{Bmatrix} \tilde{x} \\ \tilde{y} \\ \tilde{z} \end{Bmatrix} = [T] \begin{Bmatrix} x - x_o \\ y - y_o \\ z - z_o \end{Bmatrix} \quad ; \qquad \begin{Bmatrix} x \\ y \\ z \end{Bmatrix} = [T]^T \begin{Bmatrix} \tilde{x} \\ \tilde{y} \\ \tilde{z} \end{Bmatrix} + \begin{Bmatrix} x_o \\ y_o \\ z_o \end{Bmatrix}
$$

in which $[T]^T$ denotes the transpose of the matrix $[T]$.

Similarly, a vector quantity, $\bar{F}$, evaluated in the local coordinate system is transformed back to global coordinates using

$$\begin{Bmatrix} F_x \\ F_y \\ F_z \end{Bmatrix} = \begin{bmatrix} T \end{bmatrix}^T \begin{Bmatrix} \tilde{F}_x \\ \tilde{F}_y \\ \tilde{F}_z \end{Bmatrix}$$

in which $\tilde{F}_x$, $\tilde{F}_y$ and $\tilde{F}_z$ are the $\tilde{x}$, $\tilde{y}$ and $\tilde{z}$ components in local coordinates and F_x, F_y and F_z are the corresponding components in the global system.

FORMULAS FOR EVALUATING INTEGRALS INVOLVING 1/R AND 1/R'

The terms of Eq. 44 which involve 1/R and 1/R' are evaluated as follows, using the panel geometry defined by Fig. 1b.
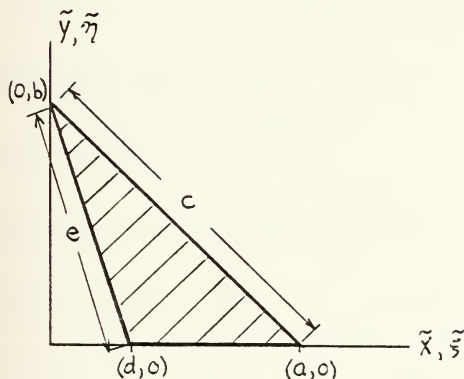
Figure 1b- Panel Geometry

$$
\iint_{\Delta S} \frac{-bd + b\tilde{\xi} + d\tilde{\eta}}{4\pi \, b(a-d) \, R} = \frac{1}{2b(a-d)4\pi} \left\{ 2\rho'\tilde{z}\,\hat{T} + d\,R_{ad} + \right.
$$

$$
(b^2 + ad)F_{ab}/c^2 - F_{db} + \left[2\rho\rho' - (b^2 + ad)(\tilde{z}^2 + \frac{\rho^2}{c^2})\right]I_{ab}^+/c
$$

$$
+ e(\tilde{z}^2 - \frac{\rho'^2}{e^2})I_{db}^+ - \left[2\tilde{y}\rho' - d(y^2 + \tilde{z}^2)\right]I_{ad}^+
$$

$$\iint_{\Delta s} \frac{ba - b\tilde{\xi} - a\tilde{\eta}}{4\pi b(a-d)R}\,ds = \frac{1}{2b(a-d)4\pi}\left\{-2\rho\tilde{z}\,\hat{T} - a\,R_{ad}\right.$$

$$+(b^2 + ad)F_{db}/e^2 - F_{ab} + [2\rho\rho' - (b^2+ad)(\tilde{z}^2 + \frac{\rho'^2}{e^2})]I_{db}^+/e$$

$$+c(\tilde{z}^2 - \frac{\rho^2}{c^2})I_{ab}^+ + [2\gamma p - a(\tilde{y}^2 + \tilde{z}^2)]I_{ad}^+\left.\right\}$$

$$\iint_{\Delta s} \frac{\tilde{\eta}}{4\pi bR}\,ds = \frac{1}{2b4\pi}\left\{2\tilde{y}\tilde{z}\,\hat{T} + R_{ad} + a\,F_{ab}/c^2 - d\,F_{db}/e^2\right.$$

$$+ [2\tilde{y}\rho - a(\tilde{z}^2 + \frac{\rho^2}{c^2})]I_{ab}^+/c - (\tilde{y}^2 - \tilde{z}^2)I_{ad}$$

$$- [2\tilde{y}\rho' - d(\tilde{z}^2 + \frac{\rho'^2}{e^2})]I_{db}^+/e$$

in which the following definitions are applicable

$$r_a = \sqrt{(\tilde{x}-a)^2 + \tilde{y}^2 + \tilde{z}^2} \qquad\qquad e = \sqrt{d^2 + b^2}$$

$$r_b = \sqrt{\tilde{x}^2 + (\tilde{y}-b)^2 + \tilde{z}^2} \qquad\qquad c = \sqrt{a^2 + b^2}$$

$$r_d = \sqrt{(\tilde{x}-d)^2 + \tilde{y}^2 + \tilde{z}^2}$$

$$\rho = b\tilde{x} + a\tilde{y} - ab \qquad\qquad \rho' = b\tilde{x} + d\tilde{y} - db$$

$$\rho_a = a\tilde{x} - b\tilde{y} - a^2 \qquad\qquad \rho_d' = d\tilde{x} - b\tilde{y} - d^2$$

$$\rho_b = a\tilde{x} - b\tilde{y} + b^2 \qquad\qquad \rho_b' = d\tilde{x} - b\tilde{y} + b^2$$

$$\hat{T} = -\tan^{-1}\left[\frac{a r_b^2 - \tilde{x}\rho_o}{\tilde{z}b\,r_b}\right] + \tan^{-1}\left[\frac{a r_a^2 - (\tilde{x}-a)\rho_a}{\tilde{z}b\,r_a}\right]$$

$$+ \tan^{-1}\left[\frac{d r_b^2 - \tilde{x}\rho_o}{\tilde{z}b\,r_b}\right] - \tan^{-1}\left[\frac{d r_d^2 - (\tilde{x}-d)\bar{\rho}_d}{\tilde{z}b\,r_d}\right]$$

$$I_{ad}^{\pm} = \log\left[r_a \pm (\tilde{x}-a)\right]/\left[r_d \pm (\tilde{x}-d)\right]$$

$$I_{ab}^{\pm} = \log\left[(c r_a \pm \rho_a)/(c r_b \pm \rho_b)\right]$$

$$I_{db}^{\pm} = \log\left[(e r_d \pm \rho_d')/(e r_b \pm \rho_o')\right]$$

47

$$R_{ad} = r_a\,(\tilde{x}-a) - r_d\,(\tilde{x}-d) \qquad\qquad I_{db}^{+} = -I_{db}^{-}$$

$$F_{ab} = \rho_b\, r_b - \rho_a\, r_a \qquad\qquad\qquad I_{ab}^{+} = -I_{ab}^{-}$$

$$F_{db} = \rho_b'\, r_b - \rho_d'\, r_d \qquad\qquad\qquad I_{ad}^{+} = -I_{ad}^{-}$$

Formulas for evaluating the terms of Eq. 45 which involve the gradients of the 1/R and 1/R' integrals are given by Webster [Ref. 10] as

$$\iint_{\Delta S} \frac{-bd+b\,\tilde{\tilde{\xi}}+d\,\tilde{\eta}}{4\pi b\,(a-d)}\,\frac{\partial}{\partial \tilde{x}}\left(1/R\right)ds = \left\{ \tilde{y}\frac{I_{ad}^{-}+\tilde{z}\,\hat{T}}{a-d} - \frac{b}{c^2}(r_a-r_b) \right.$$

$$\left. + \left[\frac{\rho}{c\,(a-d)}+\frac{b\,\rho_\rho}{c^3}\right]I_{ab}^{+} - \frac{\rho'I_{db}^{+}}{e\,(a-d)} \right\}$$

$$\iint_{\Delta S} \frac{ba-b\,\tilde{\tilde{\xi}}-a\,\tilde{\eta}}{4\pi b\,(a-d)}\,\frac{\partial}{\partial \tilde{x}}\left(1/R\right)ds = \left\{ \frac{-\tilde{y}\,I_{ad}^{-}+\tilde{z}\,\hat{T}}{(a-d)} - \frac{b}{e^2}(r_b-r_d) \right.$$

$$\left. + \left[\frac{\rho'}{e\,(a-d)}-\frac{b\,\rho_b'}{e^3}\right]I_{db}^{+} - \frac{\rho\,I_{ab}^{+}}{c\,(a-d)} \right\}$$

$$\iint_{\Delta S} \frac{\tilde{\eta}}{4\pi b}\,\frac{\partial}{\partial \tilde{x}}\left(1/R\right)ds = \left\{ \frac{b}{c^2}(r_a-r_b)+\frac{b}{e^2}(r_b-r_d)-b\left[\frac{\rho_a}{c^3}I_{ab}-\frac{\rho_d'}{e^3}I_{db}^{+}\right]\right\}$$

$$\iint_{\Delta S} \frac{-bd+b\,\tilde{\tilde{\xi}}+d\,\tilde{\eta}}{4\pi b\,(a-d)}\,\frac{\partial}{\partial \tilde{y}}\left(1/R\right)ds = \left\{ \frac{\rho'I_{ad}^{-}+d\,\tilde{z}\,\hat{T}}{b\,(a-d)} - \frac{a}{c^2}(r_a-r_b) \right.$$

$$\left. + \frac{r_a-r_d}{a-d} + \left[\frac{a\,\rho_b}{c^3}+\frac{d\,\rho}{bc\,(a-d)}\right]I_{ab}^{+} - \frac{d\rho'I_{db}^{+}}{be\,(a-d)} \right.$$

48

$$\iint_{\Delta S} \frac{ba - b\tilde{\xi} - a\tilde{\eta}}{4\pi b(a-d)} \frac{\partial}{\partial \tilde{y}}(1/R)ds = \left\{ -\left(\frac{\rho I_{ad}^- + a\tilde{z}\hat{T}}{b(a-d)} - \frac{d}{e^2}(r_b - r_d)\right)\right.$$

$$\left. -\frac{(r_a - r_d)}{a-d} - \left[\frac{d\rho'_{_3}}{e^3} - \frac{a\rho'}{be(a-d)}\right]I_{db}^+ - \frac{a\rho I_{ab}^+}{bc(a-d)}\right\}$$

$$\iint_{\Delta S} \frac{\eta}{4\pi b} \frac{\partial}{\partial \tilde{y}}(1/R)ds = \left\{\frac{\tilde{y} I_{ad}^- + \tilde{z}\hat{T}}{b} + \frac{d}{e^2}(r_b - r_1) + \frac{a}{c^2}(r_a - r_b)\right.$$

$$\left. + \left[\frac{b\rho}{c^3} + \frac{a\tilde{y}}{bc}\right]I_{ab}^+ - \left[\frac{b\tilde{\rho}}{e^3} + \frac{d\tilde{y}}{be}\right]I_{db}^+\right\}$$

$$\iint_{\Delta S} \frac{-bd + b\tilde{\xi} + d\tilde{\eta}}{4\pi b(a-d)} \frac{\partial}{\partial \tilde{z}}(1/R)ds = \frac{1}{b(a-d)}\left\{\rho'\hat{T} - \frac{ad+b^2}{c}\tilde{z}I_{ab}^+ + e\tilde{z}I_{db}\right.$$

$$\left. -d\tilde{z}I_{ad}^-\right\}$$

$$\iint_{\Delta S} \frac{ba - b\tilde{\xi} - a\tilde{\eta}}{4\pi b(a-d)} \frac{\partial}{\partial \tilde{z}}(1/R)ds = \frac{1}{b(a-d)}\left\{-\rho\hat{T} - \frac{(ad+b^2)}{e}\tilde{z}I_{db}^+\right.$$

$$\left. +c\tilde{z}I_{ab}^+ + a\tilde{z}I_{ad}^-\right\}$$

$$\iint_{\Delta S} \frac{\tilde{\eta}}{4\pi b} \frac{\partial}{\partial z}(1/R)ds = \frac{1}{b}\left\{\tilde{y}\hat{T} - \frac{a\tilde{z}}{c}I_{ab}^+ + \frac{d\tilde{z}}{e}I_{db}^- - \tilde{z}I_{ad}^-\right\}$$

FORMULAS FOR INTEGRATION OF LINEAR FUNCTIONS OVER TRIANGULAR
AREAS

All formulas given are applicable for a triangle
positioned as shown in Fig. 1c, with a>d and b>0.
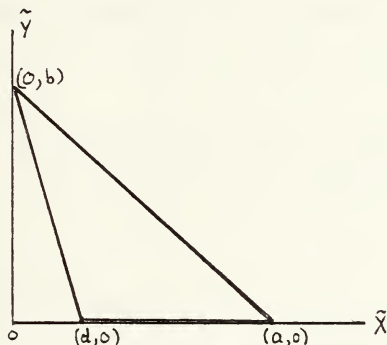
Figure 1c- Triangle Geometry

If $f(\tilde{x},\tilde{y})$ and $g(\tilde{x},\tilde{y})$ are any linear functions expressed
as

$$f(\tilde{x},\tilde{y}) = \alpha + \beta \tilde{x} + \gamma \tilde{y}$$

$$g(\tilde{x},\tilde{y}) = \alpha' + \beta' \tilde{x} + \gamma' \tilde{y}$$

and the function values at the triangle corners are denoted

by f_a, f_b, f_d, g_a, g_b, g_d, then:

$$\alpha = \frac{a f_d - d f_a}{a - d} \qquad\qquad \alpha' = a g_d - g_a d$$

$$\beta = \frac{f_a - f_d}{a - d} \qquad\qquad \beta' = g_a - g_d$$

$$\gamma = \frac{(a-d) f_b - a f_d + d f_a}{b(a-d)} \qquad\qquad \gamma' = \frac{(a-d) g_b - a g_d + d g_a}{b(a-d)}$$

and the integrals of $f(x,y)\,ds$ and $f(x,y)\,g(x,y)\,ds$ are given by

$$\iint_S f(\tilde{x}, \tilde{y}) \, ds = \frac{(f_a + f_b + f_d)}{3} W_1$$

and

$$\iint_S f(\tilde{x}, \tilde{y}) \, g(\tilde{x}, \tilde{y}) \, ds = \alpha \alpha' W_1 + (\beta \alpha' + \alpha \beta') W_2$$

$$+ (\alpha' \gamma + \alpha \gamma') W_3 + (\gamma \beta' + \beta \gamma') W_4 + \beta \beta' W_5 + \gamma \gamma' W_6$$

where

$$W_1 = \iint_S ds = \frac{(a-d) b}{2}$$

$$W_2 = \iint_S \tilde{x} \, ds = \frac{(a^2 - d^2) b}{6}$$

$$W_3 = \iint_s \tilde{y}\, ds = \frac{(a-b)b^2}{6}$$

$$W_4 = \iint_s \tilde{x}\hat{y}\, ds = \frac{b^2(a^2-d^2)}{24}$$

$$W_5 = \iint_s \tilde{x}^2 ds = \frac{(a^2+d^2+ad)(a-d)\, b}{12}$$

$$W_6 = \iint_s \tilde{y}^2 ds = \frac{b^3(a-d)}{12}$$

INTEGRATICN FORMULAS FOR INTEGRALS INVOLVING G* AND ∇G*

The assumption of a linear variation of $G*(\xi, \eta; x, y, z)$ over a given triangular panel, and the subsequent application of the formula for the integral of the product of two linear functions, given in Appendix C, leads to the following expressions for Eqs. 47 and 48 which involve the G* term. (refer to Fig. 1b for applicable triangle geometry.)

$$\iint_{\Delta s} \frac{-bd + b\tilde{\xi} + d\tilde{\eta}}{4\pi b(a-d)} G* ds = \frac{1}{4\pi(a-d)^2} \left[C_1 A_1 + C_2 A_2 + C_3 A_3 \right]$$

$$\iint_{\Delta s} \frac{ba + b\tilde{\xi} - a\tilde{\eta}}{4\pi b(a-d)} G* ds = \frac{1}{4\pi(a-d)^2} \left[C_1 B_1 + C_2 B_2 + C_3 B_3 \right]$$

$$\iint_{\Delta s} \frac{\eta}{4\pi b} G* ds = \frac{1}{4\pi b(a-d)} \left[C_1 D_1 + C_2 D_2 + C_3 D_3 \right]$$

in which

$$C_1 = G_a^* - G_d^*$$

$$C_2 = \left[(a-d) G_b^* - a G_d^* + d G_a^* \right] / b$$

$$C_3 = \left[a G_d^* - d G_a^* \right]$$

$$A_1 = \frac{b(2a-d)}{24} \qquad A_2 = \frac{b^2}{24} \qquad A_3 = \frac{b}{6}$$

$$B_1 = \frac{(a+d)b}{24} \qquad B_2 = \frac{b^2}{12} \qquad B_3 = \frac{b}{6}$$

$$D_1 = \frac{b(2d+a)}{24} \qquad D_2 = \frac{b^2}{24} \qquad D_3 = \frac{b}{6}$$

The integrations involving the gradients of G* similarly result in the following expressions:

$$\iint_{\Delta S} \frac{-bd + b\tilde{\xi} + d\tilde{\eta}}{4\pi b(a-d)} \nabla G^* ds = \frac{1}{4\pi(a-d)^2} \left[(\nabla C_1) A_1 + (\nabla C_2) A_2 + (\nabla C_3) A_3 \right]$$

$$\iint_{\Delta S} \frac{ba + b\tilde{\xi} - a\tilde{\eta}}{4\pi b(a-d)} \nabla G^* ds = \frac{1}{4\pi(a-d)^2} \left[(\nabla C_1) B_1 + (\nabla C_2) B_2 + (\nabla C_3) B_3 \right]$$

$$\iint_{\Delta S} \frac{\eta}{4\pi b} \nabla G^* ds = \frac{1}{4\pi b(a-d)} \left[(\nabla C_1) D_1 + (\nabla C_2) D_2 + (\nabla C_3) D_3 \right]$$

where

$$\nabla C_1 = \bar{i} \frac{\partial G^*(a,0)}{\partial x} + \bar{j} \frac{\partial G^*(a,0)}{\partial y} + \bar{k} \frac{\partial G^*(a,0)}{\partial z}$$

$$\qquad - \bar{i} \frac{\partial G^*(d,0)}{\partial x} - \bar{j} \frac{\partial G^*(d,0)}{\partial y} - \bar{k} \frac{\partial G^*(d,0)}{\partial z}$$

$$\nabla C_2 = \left[(a-d)\left(\bar{i} \frac{\partial G^*(0,b)}{\partial x} + \bar{j} \frac{\partial G^*(0,b)}{\partial y} + \bar{k} \frac{\partial G^*(0,b)}{\partial z} \right) - \right.$$

$$a\left(\bar{i} \frac{\partial G^*}{\partial x}(d,o) + \bar{j} \frac{\partial G^*}{\partial y}(d,o) + \bar{k} \frac{\partial G^*}{\partial z}(d,o) \right)$$

$$+ d\left(\bar{i} \frac{\partial G^*}{\partial x}(a,o) + \bar{j} \frac{\partial G^*}{\partial y}(a,o) + \bar{k} \frac{\partial G^*}{\partial z}(a,o) \right) \Big] \Big/ b$$

$$\nabla C_3 = \Big[a\left(\bar{i} \frac{\partial G^*}{\partial x}(d,o) + \bar{j} \frac{\partial G^*}{\partial y}(d,o) + \bar{k} \frac{\partial G^*}{\partial z}(d,o) \right)$$

$$- d\left(\bar{i} \frac{\partial G^*}{\partial x}(a,o) + \bar{j} \frac{\partial G^*}{\partial y}(a,o) + \bar{k} \frac{\partial G^*}{\partial z}(a,o) \right) \Big]$$

Fig.-1- Problem Definition
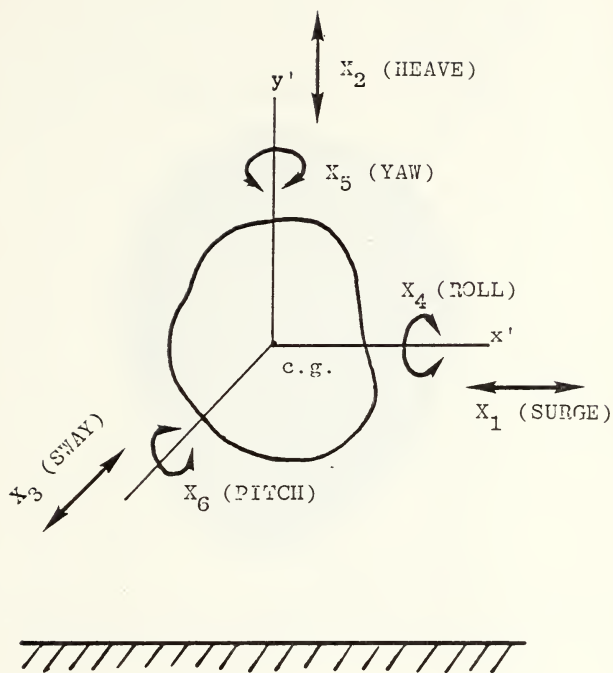
Fig. 2- Definition of Body Motion

$$\phi = \int_S f(\xi, \eta, \zeta) G(\xi, \eta, \zeta; x, y, z) ds$$
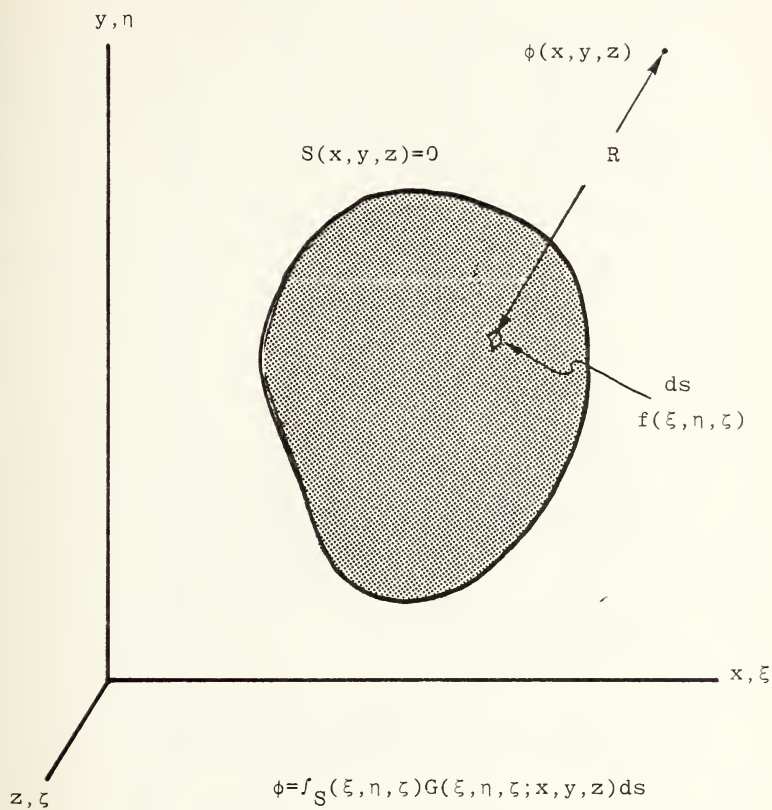
Fig. 3- Potential Due to Distributed
Sources
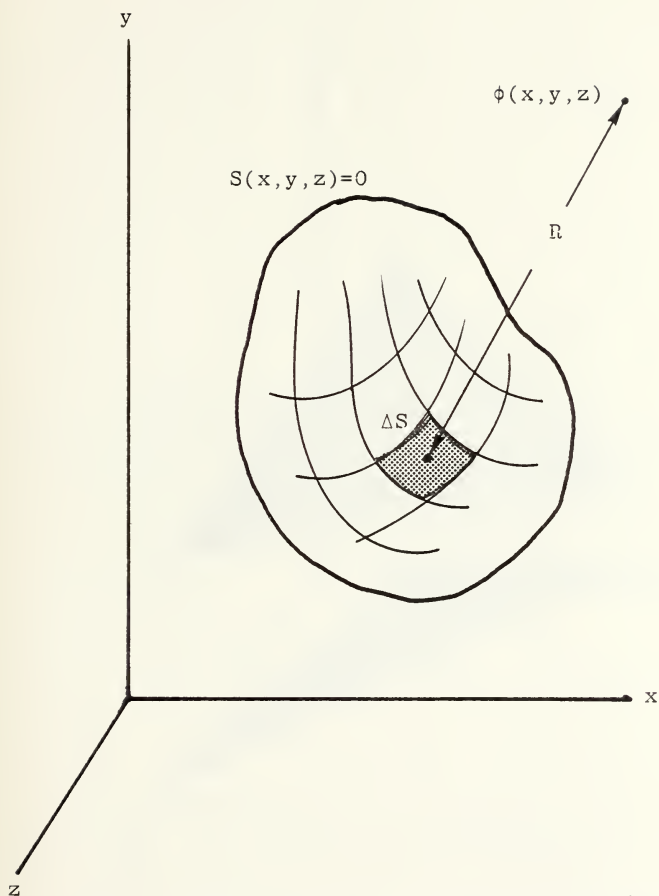
Fig. 4- Uniform Source Strength Discretization
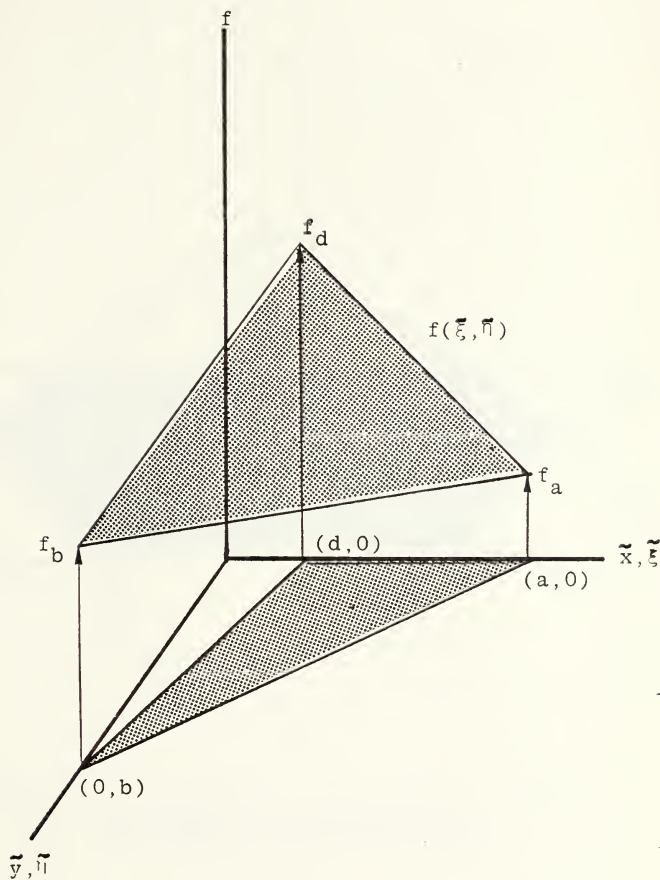
Fig. 5- Panel of Linearly Varying Source
Strength
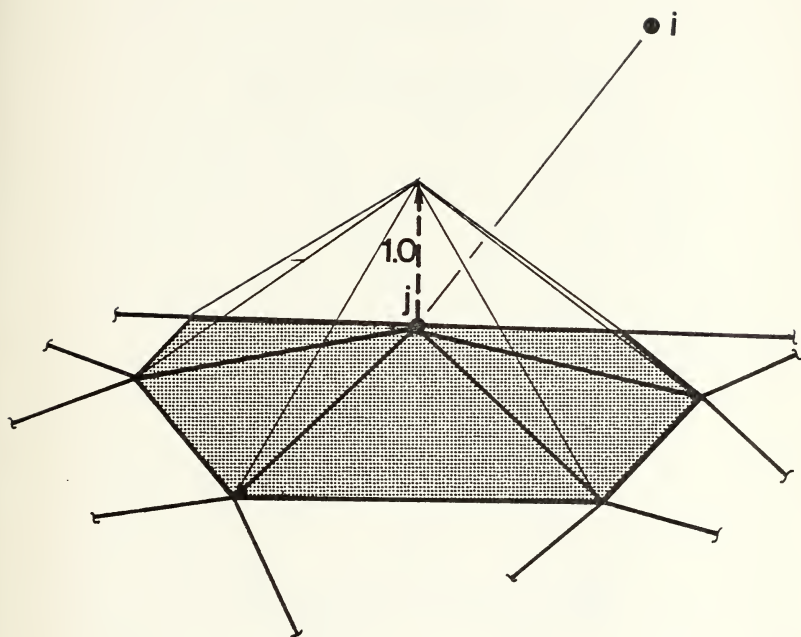
Fig. 6- Contribution to Potential at Node i
From Panels Surrounding Node j
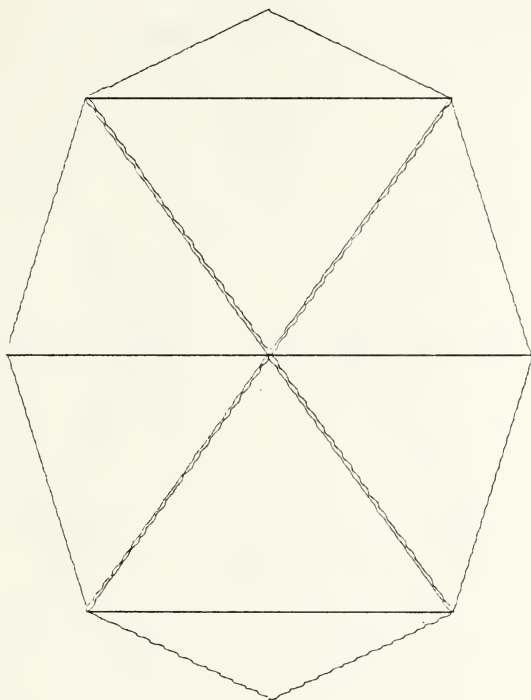
Figure   7 -   QUARTER OF A 13 NODE HEMISPHERE
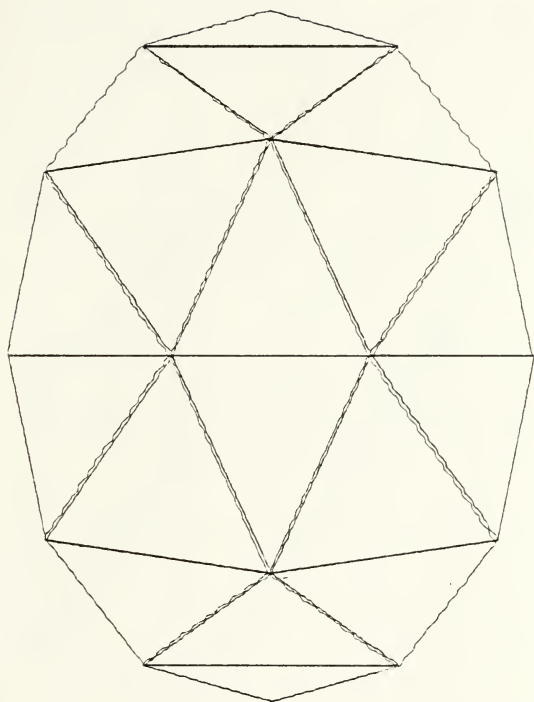
Figure   8 -   QUARTER OF A 25 NODE HEMISPHERE
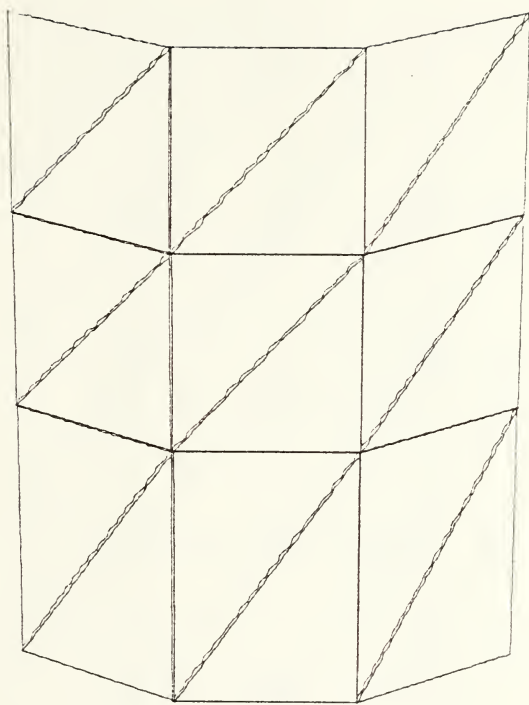
Figure   9 -   QUARTER OF A 48 NODE CIRCULAR CYLINDER
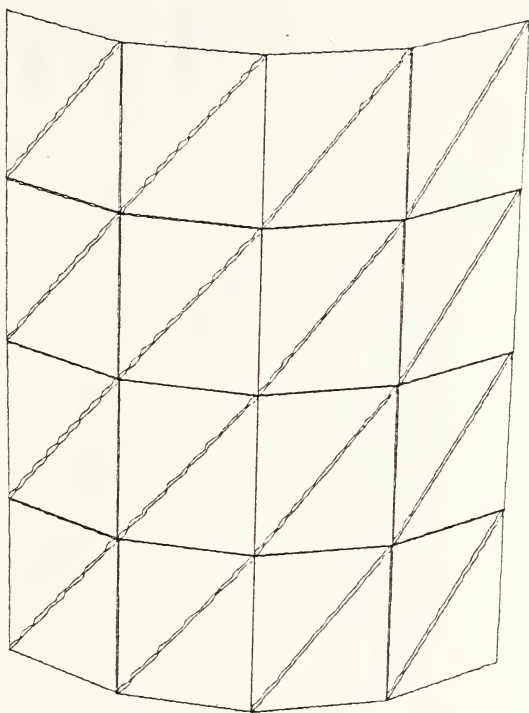
Figure 10 - QUARTER OF AN 80 NODE CIRCULAR CYLINDER
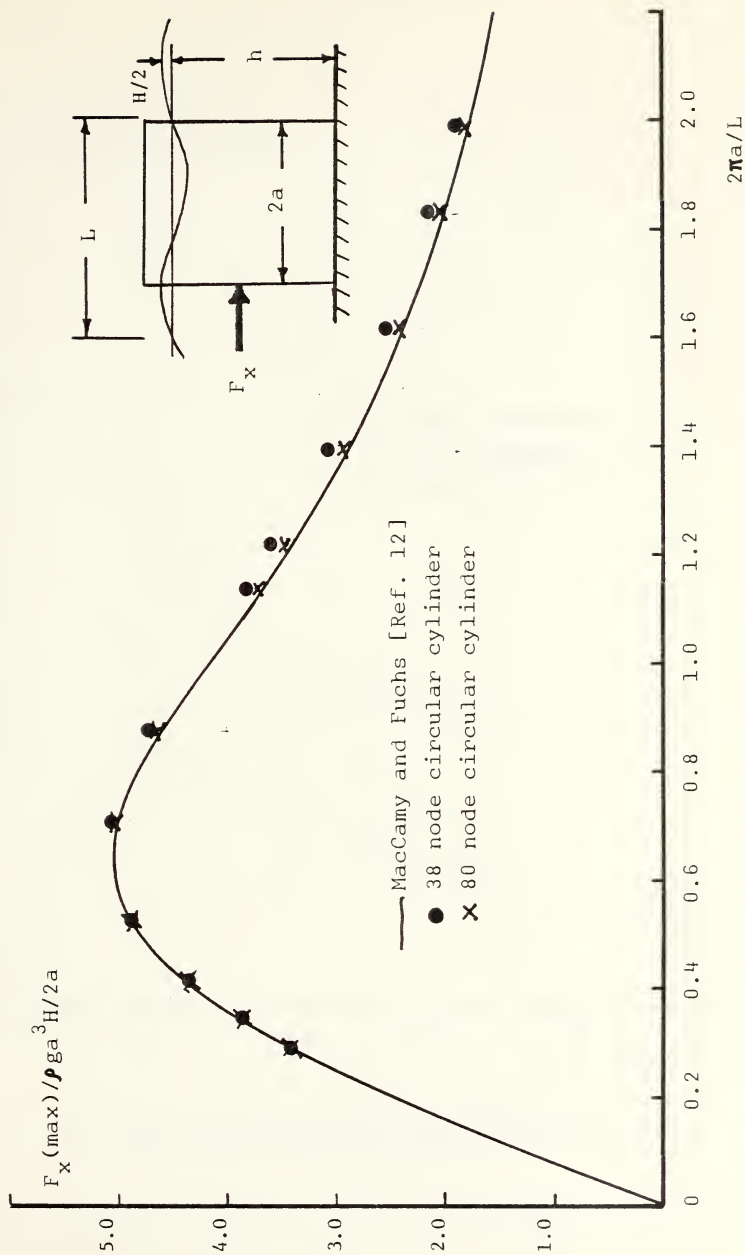
Fig. 11- Horizontal Force on a Circular Cylinder
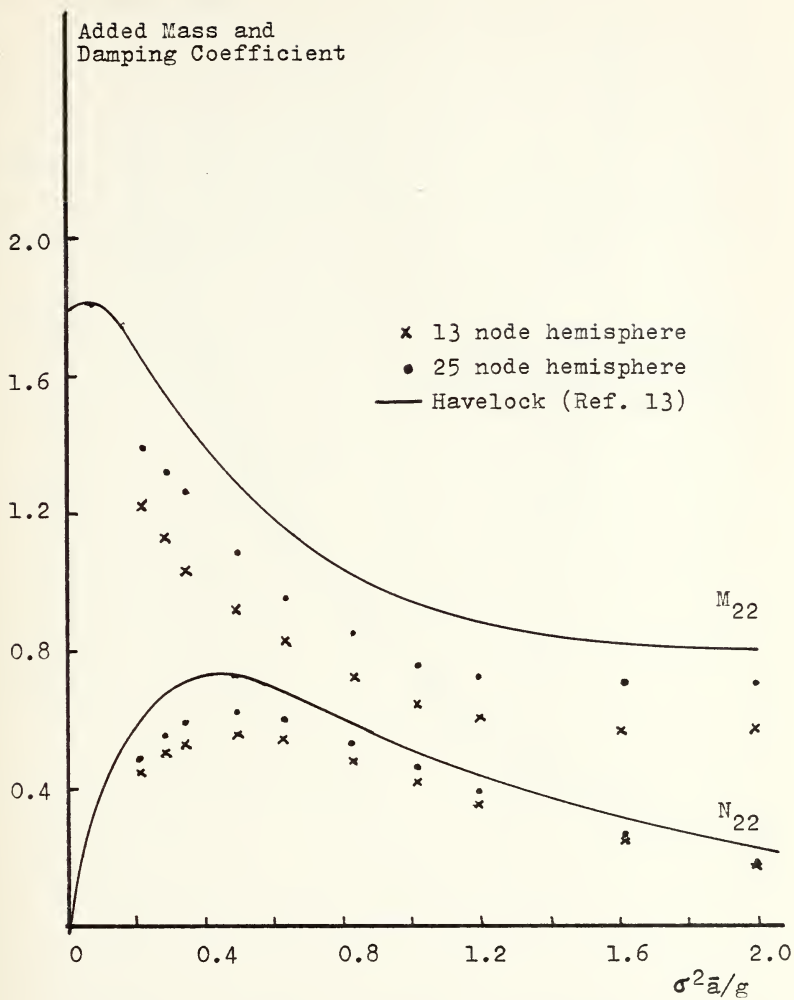
Fig. 12– Heave Added Mass and Damping Coefficients
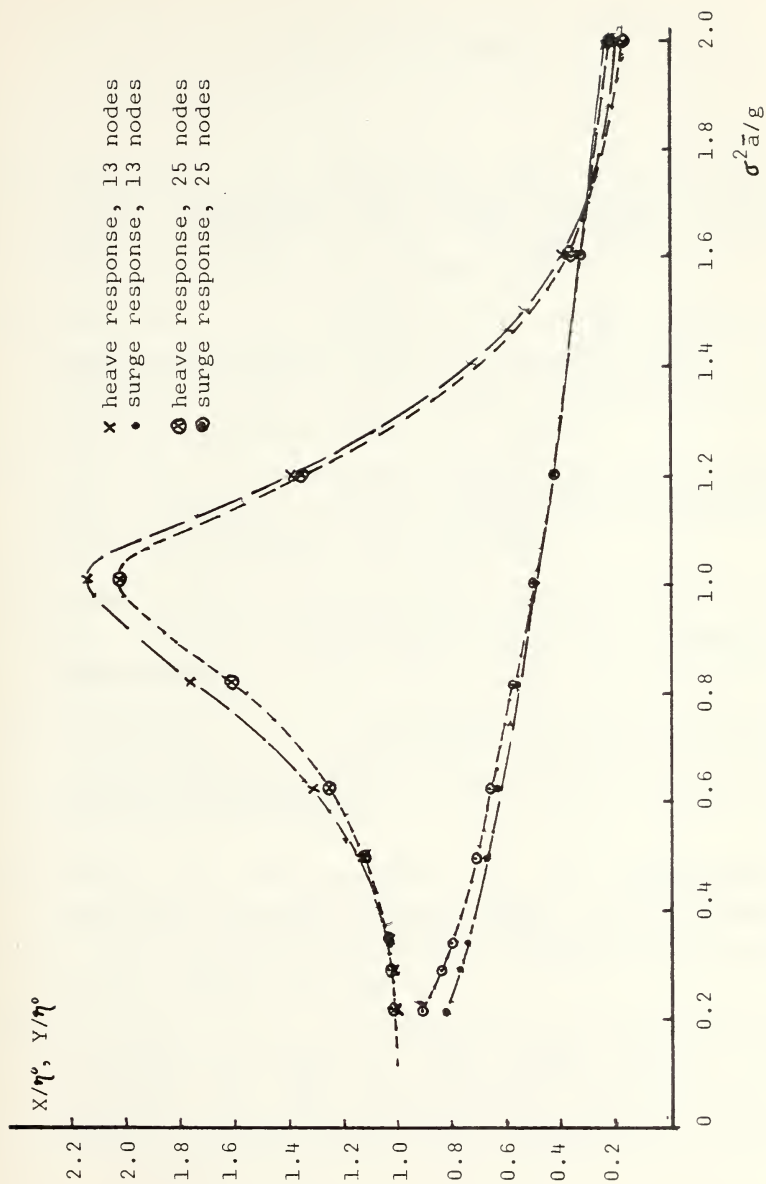for a Floating Hemisphere
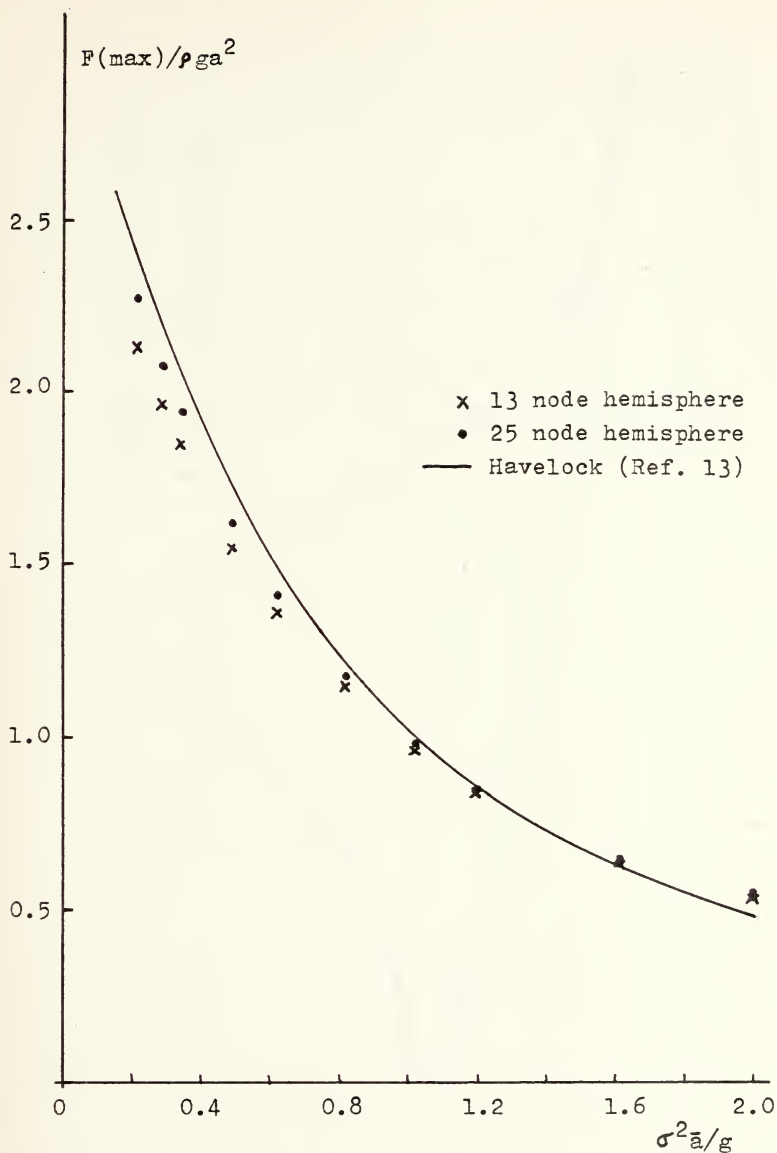
Fig. 13- Heave Excitation Force for a Floating
Hemisphere

Fig. 14- Heave and Surge Response for a Semi-immersed Sphere

x heave response, 13 nodes
• surge response, 13 nodes
⊗ heave response, 25 nodes
◉ surge response, 25 nodes

$X/\eta°$, $Y/\eta°$

$\sigma^2 \bar{a}/g$

LIST OF REFERENCES

1. Garrison, C. J., Seetharama Rao, V. and Snider, R.
    H.,_Wave Interaction with Large Submerged Objects,_
    paper presented at the Second Annual Offshore
    Technology Conference, Houston, Texas, April 1970.

2. Garrison, C. J. and Chow, P. V., _Forces Exerted on a
    Submerged Oil Storage Tank by Surface Waves_, paper
    presented at the Fourth Annual Offshore Technology
    Conference, Houston, Texas, May 1972.

3. Garrison, C. J. _Dynamic Response of Floating Bodies,_
    paper presented at the Sixth Annual Offshore Technology
    Conference, Houston, Texas, May 1974.

4. Garrison, C. J., "Hydrodynamics of Large Objects in the
    Sea, Part I-- Hydrodynamic Analysis", _Journal of
    Hydronautics_, v. 8, No. 1, p. 5-12, January 1974.

5. Garrison, C. J., " Hydrodynamics of Large Objects in
    the Sea, Part II --Motion of Free-Floating Bodies",
    Journal of Hydronautics, v. 9, No. 2, p. 58-63, April
    1975.

6. Hogben, N., and Standing, R. G., _Experience in
    Computing Wave Loads on Large Bodies_, paper presented
    at the Seventh Annual Offshore Technology Conference,
    Houston, Texas, May 1975.

7. Faltinsen, O. M. and Michelsen, F. C. _Motion of Large
    Structures in Waves at Zero Froude Number_, paper
    presented at the International Symposium on the
    Dynamics of Marine Vehicles and Structures in Waves,

University College, London, April 1974.

8. Garrison, C. J. Hydrodynamic Loading of Large Offshore Structures, paper presented at the International Symposium for Numerical Methods of Offshore Engineers, University of Swansea, Wales, U. K., January 1977.

9. Garrison, C. J., Wave Loads on North Sea Gravity Platforms: A Comparison of Theory and Experiment, paper presented at the Ninth Annual Offshore Technology Conference, Houston, Texas, May 1977.

10. Webster, W. C., "The Flow About Arbitrary, Three-Dimensional Smooth Bodies", Journal of Ship Research, v. 19 No. 4, p. 206-218, December 1975.

11. Yeung, R. W., and Bai, K. J., Numerical Solutions to Free Surface Flow Problems, paper presented at the Tenth Symposium of Naval Hydrodynamics, Massachusetts Institute of Technology, June 1974.

12. MacCamy, R. C., and Fuchs, R. A., "Wave Forces on a Pile: a Diffraction Theory," Technical Memo. 69, U.S. Army Corps of Engineers Beach Erosion Board, Washington, D.C., 1954

13. Havelock, T., "Waves Due To a Floating Sphere Making Periodic Heaving Oscillations", Proceedings of the Royal Society, London, v. 231, Ser. A, p. 1-7, 1955.

INITIAL DISTRIBUTION LIST